

PRO and SWRO experimental synergy: a renewable nexus in the Caribbean

Anggie Cala¹, Ricardo Mejía Marchena¹, Aymer Maturana Córdoba¹.

1. Universidad del Norte

Keywords— Design of Experiments, Hybrid Process, Membrane Technologies, Power Density, Pressure Retarded Osmosis, Synergies.

I. INTRODUCTION

Seawater desalination through reverse osmosis (RO) has emerged as a global solution to meet the escalating demand for water, particularly in regions grappling with freshwater scarcity [1], [2]. Despite its widespread adoption, challenges such as membrane fouling susceptibility and high energy demands persist, fueled predominantly by fossil fuels [3], [4], [5]. The current specific energy requirements for RO seawater desalination, ranging from 1.5 to 4 kWh/m³, contribute to elevated operational costs [6].

Efforts to enhance operational efficiency have focused on innovative membrane materials, energy-efficient processes, and effective pretreatment methods [7], [8], [9], [10]. Despite advancements, the economic costs of seawater desalination remain high, prompting exploration into alternative technologies.

One promising avenue involves coupling reverse osmosis with Pressure Retarded Osmosis (PRO), a process generating electricity by mixing fluids with different salinity concentrations [11], [12]. This coupling aims to co-produce water and energy, reduce process costs, and utilize brine resulting from the RO process. Integration of RO and PRO technologies has demonstrated increased energy generation, potentially producing up to 50% more water than conventional systems [13], [14], [15]. However, large-scale commercial implementation requires further research and development [16], [17], [18].

Various studies have explored the potential of RO-PRO hybrid systems, highlighting benefits in water and energy management, energy savings, and environmental advantages [14], [16], [19], [20], [21], [22], [23]. These findings emphasize the relevance and potential of hybrid RO-PRO systems in desalination, providing a glimpse into their practical application.

In a pilot plant using RO brine, attractive long-term operating costs were achieved with average power densities ranging from 1.1 to 2.3 W/m² [24]. Various RO-PRO configurations have been assessed, revealing

sensitivity in energy costs when coupled with seawater RO [19]. Combining RO/PRO demonstrated a reduction in RO input power by up to 38% [25]. However, a different study reported 50% higher energy consumption in RO-PRO compared to two-stage RO [14]

Noteworthy RO/PRO projects include the Mega-ton hybrid plant in Japan and the Korean Global MVP project. Using treated freshwater and RO brine, Mega-ton achieved a maximum power output of 13.8 W/m² [26]. The Korean project, employing MED, RO, and PRO, reduced brine by 30% and produced a power density of 7.5 W/m² [27], aiming to recover energy and water from brine. Some authors propose that the hybrid RO-PRO configuration is advantageous in seawater applications compared to PRO-RO, citing the use of RO brine as a draw solution in PRO, leading to a more significant salt difference and improved overall energy efficiency. Additional factors include produced water quality, energy cost reduction, design flexibility, membrane wellness, and waste management [28] Therefore, this study uniquely examines produced water quality and energy cost reduction on a lab scale.

In the complex scenario of the Colombian Caribbean, this work embarks on an ambitious endeavor: the experimental assessment of seawater desalination by RO and salinity gradient energy (SGE) production by PRO technology. While RO/PRO experimentation is established, the Colombian Caribbean conditions present a new frontier for these technologies due to regional water quality, site-specific potential, and local service costs. Moreover, the Caribbean Region confronts formidable water and energy supply challenges, with irregular access to potable water and a growing demand for non-renewable sources [29], [30].

The drinking water supply, solely dependent on the Magdalena River, must be revised, particularly during emergencies like river spills [31]. Amid these challenges, the prospect of integrating seawater desalination and SGE through RO/PRO technology emerges as a paradigm-shifting opportunity, considering the unprecedented potential for harnessing sustainable energy and freshwater resources in this region [32].

This study provides detailed information on two proposed lab-scale configurations between RO and PRO (RO-PRO and PRO-RO), offering a comprehensive initial view of these technologies through methodical

experimental design, statistical analysis, and power density estimations using natural water samples. The results enable a comparison of configurations, and upon evaluating criteria encompassing energetic, water production quality, and synergic performances, the suggested option for the region's conditions is determined.

II. METHODS

The methods used in this investigation, which include essential elements such as Sampling and characterization, Pretreatment, PRO Membrane characterization and other estimations, are fully described in this section.

A. Sampling and characterization

This study, conducted at coordinates 11°04'55.8" N, 74°50'50.4"W along the Magdalena River and 11°04'37.6" N, 74°50'53.8"W in the Caribbean Sea at Bocas de Ceniza, involves collecting composite water samples. Essential parameters like temperature, turbidity, conductivity, pH, and Total Dissolved Solids (TDS) are measured using a Hanna 9829 multi-parameter probe. With minimal variation in these measurements, the study assesses the water samples' fouling propensity through SDI measurements and determines Total Organic Content (TOC) using HACH TNT 810 vials. Method 10054 is applied for additional correlation [33].

B. Pretreatment

Pretreatment involved two stages: Multimedia filtration at 30 psi for seawater and surface water. Second, Ultrafiltration (UF) using flat sheet membranes in a Convertible Membrane Test Skid at 90-100 psi, with temperature control by a ½ HP Polyscience chiller.

C. PRO Membrane characterization and other estimations

In PRO, permeation through the membrane requires a driving force based on the difference in salt concentration between the solutions. Equation (1) defines water flux (J_w) in PRO considering the salt concentration difference ($\Delta\pi - \Delta P$) and membrane water permeability (A) [34].

$$J_w = A (\Delta\pi - \Delta P) \quad (1)$$

Accounting for imperfections like Internal Concentration Polarization (ICP) and External Concentration Polarization (ECP), Equation (2) introduces additional parameters [35].

$$J_w = A \left[\pi_{D,b} \exp\left(-\frac{J_w}{k}\right) \frac{1 - \frac{\pi_{f,b}}{\pi_{D,b}} \exp\left(\frac{J_w K}{K}\right) \exp\left(\frac{J_w}{K}\right)}{1 + \frac{B}{J_w} [\exp(J_w K) - 1]} - \Delta P \right] \quad (2)$$

Equations (3), (4), (5), and (6) calculate external concentration polarization modulus, mass transfer

coefficient, diffusion coefficient, and solute resistivity (K) based on Forward Osmosis (FO) experiments.

$$\frac{\pi_{f,b}}{\pi_{D,b}} = \exp\left(-\frac{J_w}{k}\right) \quad (3)$$

$$k = \left(-\frac{Sh D}{d_h}\right) \quad (4)$$

$$D = \frac{b * T}{6 * \pi * \mu * r} \quad (5)$$

$$K = \frac{1}{J_w} \ln\left(\frac{A \pi_{D,b} \exp\left(-\frac{J_w}{k}\right) - J_w}{B} + 1\right) \quad (6)$$

The osmotic pressure at the membrane surface ($\pi_{f,b}$) and the bulk osmotic pressure of the extraction solution ($\pi_{D,b}$) are crucial in evaluating water flux (J_w) in PRO. Negative J_w results from water flux into the more concentrated solution ($\pi_{f,b} < \pi_{D,b}$). The Sherwood number (Sh) is calculated using the correlation $Sh = 0.2 Re^{0.57} Sc^{0.40}$, where Re is the Reynolds number, Sc is the Schmidt number, D is the diffusion coefficient of solute in the extraction solution, and d_h is the hydraulic channel diameter. Additionally, the diffusion coefficient (D) is determined using Boltzmann's constant (b), temperature (T) in Kelvin, viscosity (μ) in kg/m*s, and particle radius (r).

To derive FTSH2O membrane coefficients, tests were conducted using a RO mode filtration system at a constant temperature of 25°C. Achilli et al. offer detailed experimental methodology and parameter calculations in [36]. The research evaluates power density (W) in PRO using Equations (7) and (8), representing energy extraction per membrane unit area. Maximum power density occurs when $\Delta P = \Delta\pi/2$, considering ICP, ECP, and reverse salt flux effects [11].

$$W = J_w \Delta P \quad (7)$$

$$W = A (\Delta\pi - \Delta P) \Delta P \quad (8)$$

Coupling configurations RO-PRO Fig. 1 illustrates the two coupled configurations proposed for this research. These were established by considering the effluents system's sequence and the effluents' salt concentration. In the quest for higher power density in PRO, surface water is chosen for its low salt concentration, aiming to amplify the salt gradient and enhance efficiency [19], [37] Two configurations are explored: in the first, pretreated seawater undergoes RO, and its brine acts as the high-salt solution for PRO. In the second, PRO precedes RO,

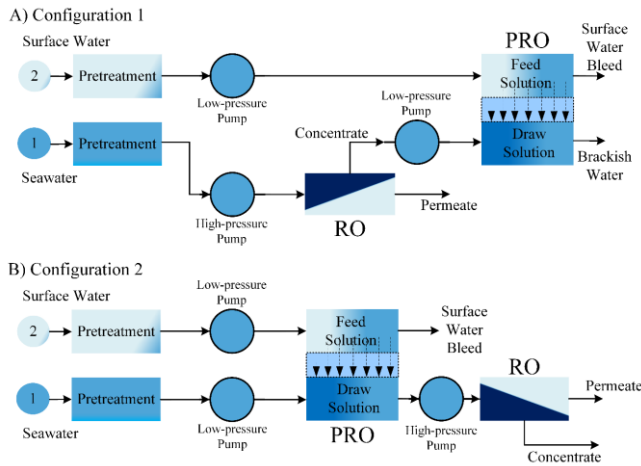


Fig.1 Schematization of the two configurations: A) RO-PRO; B) PRO-RO.

utilizing pretreated river and seawater to produce brackish water for RO desalination. Operating conditions vary for RO processes, with seawater at 700 psi and brackish water at 200 psi. The PRO process involves a custom bench with a 4 L tank for low salinity water and a 20 L polypropylene tank for high salinity water. Recirculation is managed by a variable-speed gear pump for low salinity water and a motor pump assembly with a variable frequency drive for high salinity water. Flat sheet membranes in a CF042A-FO cell, a Polyscience 1/2 HP chiller, and defined operating conditions per DoE complete the setup.

D. DoE

This study employed a fractional experiment (2x3) using JMP Pro 14 software. Each of the 36 trials, spanning 0 to 2 hours with 5-minute intervals, involved five randomly ordered replicates. Table 1 details the control and response variables.

Table 1. DoE variables: Types, definitions, code, and levels.

Variables	Type	Definition	Units	Coded level and value		
				-1	0	+1
x 1 Pressure delta (P Delta)	Control	The pressure differential between the river and seawater supply	psi	45	70	95
x 2 High salinity solution concentration (C Draw)	Control	Each configuration has a high salinity solution concentration supply, corresponding to brine and seawater.	mg/L	33.2	-	48.9
y 1 Power density (WORP)	Response	The total amount of energy that can be obtained per unit area of the membrane in the module.	W/m ²	-	-	-

Pressure gradient (45, 70, and 95 psi) and salt concentration were employed as control variables. Configuration 1 had a high salinity solution of 33,160 mg/L, while configuration 2 had 48,862 mg/L. Despite coding these variables as continuous, they were treated as qualitative for analysis, reflecting their respective configurations.

E. Selection matrix parameters

The decision matrix, with equal weights (0.3333 each) for three components, guides configuration selection:

- a. Technical PRO Component:
 - Assesses higher net energy consumption in PRO.
 - Scores assigned based on positive net consumptions using a specific equation.
- b. Water Quality Component at RO:
 - Penalizes configurations with conductivity in produced water exceeding 1000 µs/cm.
 - Water quality rating determined by an exponential equation.
- c. Synergic Coupling Component:
 - Assesses water and energy return rate (WERR) for benefits in RO water production and PRO power generation.

Equation considers parameters to reward higher gains and penalize lower incomes in configurations.

III. RESULTS & DISCUSSION

Results and discussion are provided below, following Pretreatment and Water quality sequence, Membrane characteristics and PRO coefficients, Statistical Analysis, Flux and Power Density Estimates, and Selection.).

A. Water Quality and Pretreatment

The sampling points generally exhibit stable conditions, though seasonal turbidity variations were noted between April and August 2022. Turbidity values ranged from 278 to 556 NTU (Magdalena River) and 21 to 101.3 NTU (Caribbean Sea). TDS showed typical values of 102.0 mg/L (surface water) and 35,864 mg/L (seawater). TOC, indicating organic matter, averaged 11.0 mg/L (surface water) and 20.7 mg/L (seawater). The proposed pretreatment achieved substantial reductions: 99.63% and 99.33% for turbidity and 91.00% and 76.43% for TOC in river and seawater, respectively. The SDI assessment confirms the effectiveness of the pretreatment, with values complying with the required limit of 5 for Magdalena River water. For pretreated Caribbean seawater, an adjustment to pH 6 improved SDI15 values to 3.1-3.4, ensuring suitability for the RO/PRO system.

B. Membrane characteristics and PRO coefficients

After the experimental execution described in the methodology, the characteristics A and B of the membrane, the mass transport coefficient, and the solute resistivity are determined. Membrane evaluation at varied delta pressures (50, 100, 150) showed increasing flux rates: 1.17 LMH, 2.42 LMH, and 3.7 LMH, respectively. The global average flux was 8.80199×10^{-7} m/s, estimating A for the study's membrane as 5.86799×10^{-9} (m/s)/psi. Linear flux increase with higher hydraulic pressure aligns with similar-scale evaluations (Fig 2).

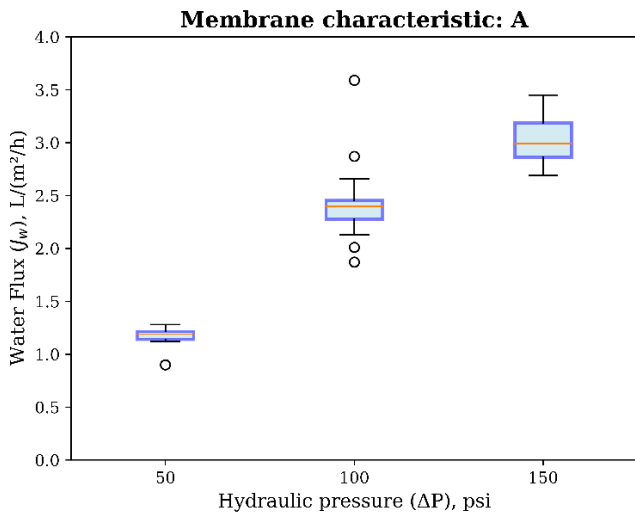


Fig. 2. Experiment to determine A, media water flux (J_w) was measured as a function of applied hydraulic pressure (ΔP) at 25°C, with DI water as the feed solution.

An initial salt rejection of 95% is calculated for the membrane, and B is determined as 6.13474×10^{-8} m/s. For k determination in Eq. 4, parameters including dh (8.68612×10^{-5} m) and concentrations were experimentally evaluated. Thickness, tortuosity, and porosity of the support layer were considered for K determination. The values of k experienced a slight increase in response to increasing concentration of the extraction solution. This phenomenon can be due to the observed increase in density, viscosity, and diffusion coefficient as the solute concentration increases [38]. These factors influence the efficiency of the extraction process and may affect the mass transfer rates involved in the system. For the theoretical flux estimates with the coefficients calculated above, the average D is set to 1.51×10^{-9} m²/s, the mass transfer coefficient $k = 9.17 \times 10^{-4}$ m/s, the membrane exhibits a structural characteristic of τ/ϵ is 2.32×10^{-3} , with the solute resistivity coefficient K being 1.54×10^6 s/m upon recalculation using Eq. 6.

C. Statistical Analysis

The ANOVA results indicate a highly significant model impact on power density, with a robust R^2 of 0.955 and adjusted R^2 of 0.95. Utilizing three degrees of freedom, the

model displays a substantial F-ratio of 50.0085, surpassing the critical value. The low probability ($\text{Prob}>F < 0.0001$) further underscores the statistical significance of the findings. The effects test in Table 2 outlines variable-specific impacts. This comprehensive analysis supports the model's effectiveness in predicting and enhancing turbidity reduction efficiency, providing a solid foundation for further improvements in the experimental setup.

Table 2. ANOVA effects test for DoE of PRO.

Source	N parameters	Degrees of freedom	Sum of squares	F Ratio	Prob>F
Delta P (psi)	1	1	12.721192	104.7086	<0.0001*
C draw (mg/L)	1	1	3.623317	29.8236	<0.0001*
Delta P (psi)*C draw (mg/L)	1	1	1.882289	15.4932	<0.0004

*Statistically significant values.

Delta P and C draw exert significant and statistically confirmed impacts on the response, with high F-ratios (104.7086 and 29.8236, respectively) and probabilities ($\text{Prob}>F$) less than 0.0001. The interaction between Delta P and C draw is also noteworthy, showing statistical significance with a probability of less than 0.0004. The adjusted model prediction is encapsulated by Eq 9.

$$\begin{aligned}
 W_{PRO} = & 1 + 0.659583333 * \left(\frac{\text{Delta P (psi)} - 70}{25} \right) \\
 & + 0.323333333 \\
 & * \left(\frac{\text{Cdraw} \left(\frac{\text{mg}}{\text{L}} \right) - 33391.5}{15470.5} \right) \\
 & + \left(\frac{\text{Delta P (psi)} - 70}{25} \right) \\
 & * \left(\frac{\text{Cdraw} \left(\frac{\text{mg}}{\text{L}} \right) - 33391.5}{15470.0} \right) \\
 & * 0.342083333
 \end{aligned} \quad (9)$$

D. Flux and Power Density Estimates

Fig. 3 depicts experimental water flux (lines) and power density (markers) under various higher hydraulic pressures. It contrasts power density from the ideal model (Wideal), disregarding concentration polarization and salt passage effects, with the theoretical model (Wteroric) considering these effects. Additionally, it includes the experimental power density from the test bench (Wexperimental). The left side presents results for configuration 1, while the right side illustrates configuration 2.

Figure 6 demonstrates a reduction in water flux and power

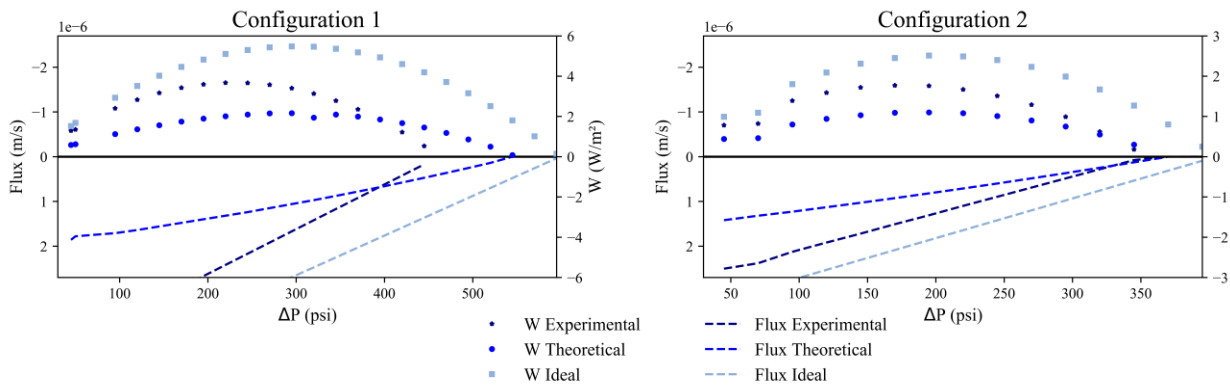


Fig. 3. Experimental and theoretical results for water flux (J_w) and power density (W) as a function of applied hydraulic pressures.

density values when applying the theoretical model due to ion concentration effects and increased salt passage resistance through the membrane. Experimental results show a lower impact of these effects, emphasizing the positive effect of process water pretreatment. In Configuration 1, the highest experimental power density reaches 3.66 W/m^2 at ΔP 245 psi, surpassing the theoretical value of 2.09 W/m^2 at ΔP 295 psi. Configuration 2 achieves a maximum experimental power density of 1.77 W/m^2 at ΔP 170 psi, exceeding the theoretical value of 1.10 W/m^2 at ΔP 195 psi. Discrepancies between calculated and experimental data in Configuration 1's PRO module stage are attributed to limitations in recorded data and physical constraints in the experimental cell.

E. Selection

Table 3 evaluation indicates Configuration 2 as the preferred choice in this lab-scale research due to negative net energy consumption and WERR values, influenced by pumps with excessive capacity for the 33.6 cm^2 membrane, with detailed hydraulic loss control beyond the study's scope.

Configuration 2 emerges as the preferred choice due to notable water quality advantages and a significant synergistic component, influenced by lower energy consumption in pumping compared to Configuration 1. The RO process dominates costs in the hybrid system, primarily driven by feed water salt concentrations. Both configurations exhibit higher energy demand than generation, associated with the small-scale evaluation. The limited influence of PRO on RO performance is attributed

to technical and synergistic aspects, with higher salt concentration differences benefiting net energy consumption and energy recovery efficiency (WERR). Notably, Configuration 2 achieves significantly lower conductivity, surpassing water quality standards and recommendations, implying lower energy consumption and greater efficiency. The WERR calculations consider local electricity costs and water prices, emphasizing their impact on evaluation results. Any variations in these prices would affect WERR values, emphasizing the significance of water pricing in the determination of WERR.

IV. CONCLUSION

This study brings forth significant findings regarding the feasibility of hybridizing RO and PRO processes:

1. Effective Pretreatment: The study successfully reduced turbidity (99.63%-99.33%) and TOC values (91.00%-76.43%) for river and seawater. The pretreatment maintained SDI below 5, ensuring optimal RO and PRO system performance.
2. FTSH2O Membrane Characterization: Crucial coefficients for energy generation estimation were obtained, including linear water flux increase with hydraulic pressure ($A: 5.86799 \times 10^{-9} \text{ (m/s)/psi}$). The mass transport coefficient (k) and solute resistivity (K) are essential for future investigations using the same membrane.

Table 3. Configuration selection matrix

Configurations		Technical Component		Water Quality Component		Synergic Component		Total
No.	Description	Net Consumption Wh/m ²	Score	Conductivity μs/cm	Score	WERR \$/h	Score	Score
1	RO in the first stage + PRO in the second stage	-4.79	1.20	986	7.72	-286	1.12	3.43
2	PRO in the first stage + RO in the second stage	-6.68	0.50	6.64	9.97	-100	3.45	4.67

3. Statistical Analysis: ANOVA revealed a highly significant effect of the model on power density ($R^2 = 0.955$). Delta P (psi) and C extraction (mg/L) significantly impacted the response, offering insights for optimizing power generation.
4. Experimental vs. Theoretical Results: Experimental data consistently outperformed theoretical predictions, emphasizing the positive impact of process water pretreatment. Configuration 1 achieved a noteworthy experimental power density of 3.66 W/m², surpassing theoretical estimates. Configuration 2 demonstrated potential with an experimental power density of 1.77 W/m².
5. Comparative Analysis: Configuration 2 emerged as the superior choice due to significantly lower conductivity, meeting water quality standards, and demonstrating noteworthy synergistic advantages.
6. Contextual Considerations: Caution is advised when extrapolating findings to other contexts due to the specific characteristics of the case. However, the study serves as a robust reference for similar research, offering a foundation for tailored analyses.
7. Gateway for Sustainable Processes: The study opens doors to comparing alternative couplings for sustainable processes, encouraging further exploration by researchers. Coupling SWRO with SGE provides a novel solution for communities facing resource scarcity, advocating for continued research and practical applications across diverse domains. Ongoing efforts focus on enhancing energy efficiency, assessing site-specific indicators, and analyzing larger-scale modules to contribute to sustainable and economically viable solutions for communities in need.

Funding: This research was funded with resources from 'PATRIMONIO AUTÓNOMO FONDO NACIONAL DE FINANCIAMIENTO PARA LA CIENCIA, LA TECNOLOGÍA Y LA INNOVACIÓN FRANCISCO JOSÉ DE CALDAS' by 'Ministerio de Ciencias, tecnología e innovación de Colombia (MINCIENCIAS)' developed under the contingent reclamation financing agreement No. 80740-538-2020.

REFERENCES

- [1] M. Ayaz, M. A. Namazi, M. A. ud Din, M. I. M. Ershath, A. Mansour, and el H. M. Aggoune, "Sustainable sea water desalination: Current status, environmental implications and future expectations," *Desalination*, vol. 540, p. 116022, Oct. 2022, doi: 10.1016/J.DESAL.2022.116022.
- [2] V. G. Gude, "Desalination and water reuse to address global water scarcity," *Rev Environ Sci Biotechnol*, vol. 16, no. 4, pp. 591–609, Dec. 2017, doi: 10.1007/S11157-017-9449-7/TABLES/5.
- [3] F. E. Ahmed, A. Khalil, and N. Hilal, "Emerging desalination technologies: Current status, challenges and future trends," *Desalination*, vol. 517, p. 115183, Dec. 2021, doi: 10.1016/J.DESAL.2021.115183.
- [4] J. Kim, K. Park, D. R. Yang, and S. Hong, "A comprehensive review of energy consumption of seawater reverse osmosis desalination plants," *Appl Energy*, vol. 254, no. April, p. 113652, 2019, doi: 10.1016/j.apenergy.2019.113652.
- [5] S. Liyanaarachchi, L. Shu, S. Muthukumaran, V. Jegatheesan, and K. Baskaran, "Problems in sea water industrial desalination processes and potential sustainable solutions: A review," *Rev Environ Sci Biotechnol*, vol. 13, no. 2, pp. 203–214, Nov. 2014, doi: 10.1007/S11157-013-9326-Y/METRICS.
- [6] A. A. Alsarayreh, M. A. Al-Obaidi, A. M. Al-Hroub, R. Patel, and I. M. Mujtaba, "Evaluation and minimisation of energy consumption in a medium-scale reverse osmosis brackish water desalination plant," *J Clean Prod*, vol. 248, p. 119220, Mar. 2020, doi: 10.1016/J.JCLEPRO.2019.119220.
- [7] A. T. Beshia, M. T. Tsehaye, D. Aili, W. Zhang, and R. A. Tufa, "Design of Monovalent Ion Selective Membranes for Reducing the Impacts of Multivalent Ions in Reverse Electrodialysis," *Membranes 2020, Vol. 10, Page 7*, vol. 10, no. 1, p. 7, Dec. 2019, doi: 10.3390/MEMBRANES10010007.
- [8] J. Kim *et al.*, "A high-performance and fouling resistant thin-film composite membrane prepared via coating TiO₂ nanoparticles by sol-gel-derived spray method for PRO applications," *Desalination*, vol. 397, pp. 157–164, Nov. 2016, doi: 10.1016/J.DESAL.2016.07.002.
- [9] S. P. Nunes *et al.*, "Thinking the future of membranes: Perspectives for advanced and new membrane materials and manufacturing processes," *J Memb Sci*, vol. 598, p. 117761, Mar. 2020, doi: 10.1016/J.MEMSCI.2019.117761.
- [10] Salinas-Rodriguez; Sergio G., Schippers; Jan C, Amy; Gay L., and Kennedy; Maria D, *Seawater Reverse Osmosis Desalination: Assessment & Pre-treatment of Fouling and Scaling*. IWA Publishing, 2021. Accessed: Nov. 05, 2022. [Online]. Available: <https://desalination-delft.nl/wp-content/uploads/2021/07/SWRO-Assessment-and-pretreatment-of-fouling-and-scaling-2021-IWA-Publishing.pdf>
- [11] S. Lanjewar, A. Mukherjee, L. Muzamil Rehman, and A. Roy, "Blue Energy and Its Potential: The Membrane Based Energy Harvesting," in *Advances in Membrane Technologies*, IntechOpen, 2020. doi: 10.5772/intechopen.86953.
- [12] N. Y. Yip, D. Brogioli, H. V. M. Hamelers, and K. Nijmeijer, "Salinity gradients for sustainable energy: Primer, progress, and prospects," *Environ Sci Technol*, vol. 50, no. 22, pp. 12072–12094, 2016, doi: 10.1021/acs.est.6b03448.

- [13] F. Esmaeilion, "Hybrid renewable energy systems for desalination," *Appl Water Sci*, vol. 10, no. 3, pp. 1–47, Mar. 2020, doi: 10.1007/S13201-020-1168-5/TABLES/11.
- [14] M. Li, "Reducing specific energy consumption of seawater desalination: Staged RO or RO-PRO?," *Desalination*, vol. 422, pp. 124–133, Nov. 2017, doi: 10.1016/J.DESAL.2017.08.023.
- [15] R. Makabe, T. Ueyama, H. Sakai, and A. Tanioka, "Commercial pressure retarded osmosis systems for seawater desalination plants," *Membranes (Basel)*, vol. 11, no. 1, pp. 1–14, Jan. 2021, doi: 10.3390/MEMBRANES11010069.
- [16] J. L. Prante, J. A. Ruskowitz, A. E. Childress, and A. Achilli, "RO-PRO desalination: An integrated low-energy approach to sea water desalination," *Appl Energy*, vol. 120, pp. 104–114, May 2014, doi: 10.1016/J.APENERGY.2014.01.013.
- [17] E. Bargiacchi, F. Orciuolo, L. Ferrari, and U. Desideri, "Use of Pressure-Retarded-Osmosis to reduce Reverse Osmosis energy consumption by exploiting hypersaline flows," *Energy*, vol. 211, p. 118969, Nov. 2020, doi: 10.1016/J.ENERGY.2020.118969.
- [18] L. Song, "Modeling and Optimization of Membrane Process for Salinity Gradient Energy Production," *Separations 2021, Vol. 8, Page 64*, vol. 8, no. 5, p. 64, May 2021, doi: 10.3390/SEPARATIONS8050064.
- [19] J. Kim, M. Park, S. Shane A., and J. H. Kim, "Reverse osmosis (RO) and pressure retarded osmosis (PRO) hybrid processes: Model-based scenario study," *Desalination*, pp. 121–130, 2013.
- [20] Q. Wang, Z. Zhou, J. Li, Q. Tang, and Y. Hu, "Investigation of the reduced specific energy consumption of the RO-PRO hybrid system based on temperature-enhanced pressure retarded osmosis," *J Memb Sci*, vol. 581, pp. 439–452, Jul. 2019, doi: 10.1016/J.MEMSCI.2019.03.079.
- [21] Y. G. Park, K. Chung, I. H. Yeo, W. I. Lee, and T. S. Park, "Development of a SWRO-PRO hybrid desalination system: pilot plant investigations," *Water Supply*, vol. 18, no. 2, pp. 473–481, Apr. 2018, doi: 10.2166/WS.2017.115.
- [22] J. M. Salamanca, O. Álvarez-Silva, and F. Tadeo, "Potential and analysis of an osmotic power plant in the Magdalena River using experimental field-data," *Energy*, vol. 180, pp. 548–555, Aug. 2019, doi: 10.1016/J.ENERGY.2019.05.048.
- [23] L. Mendoza-Zapata, A. Maturana-Córdoba, R. Mejía-Marchena, A. Cala, J. Soto-Verjel, and S. Villamizar, "Unlocking synergies between seawater desalination and saline gradient energy: Assessing the environmental and economic benefits for dual water and energy production," *Appl Energy*, vol. 351, p. 121876, Dec. 2023, doi: 10.1016/J.APENERGY.2023.121876.
- [24] A. Achilli, J. L. Prante, N. T. Hancock, E. B. Maxwell, and A. E. Childress, "Experimental results from RO-PRO: A next generation system for low-energy desalination," *Environ Sci Technol*, vol. 48, no. 11, pp. 6437–6443, Jun. 2014, doi: 10.1021/ES405556S/ASSET/IMAGES/MEDIUM/ES-2013-05556S_0008.GIF.
- [25] M. H. Sharqawy, S. M. Zubair, and J. H. Lienhard, "Second law analysis of reverse osmosis desalination plants: An alternative design using pressure retarded osmosis," *Energy*, vol. 36, no. 11, pp. 6617–6626, Nov. 2011, doi: 10.1016/J.ENERGY.2011.08.056.
- [26] K. Saito, M. Irie, S. Zaitso, H. Sakai, H. Hayashi, and A. Tanioka, "Power generation with salinity gradient by pressure retarded osmosis using concentrated brine from SWRO system and treated sewage as pure water," *New pub: Balaban*, vol. 41, no. 1–3, pp. 114–121, 2012, doi: 10.1080/19443994.2012.664696.
- [27] S. Lee, J. Choi, Y. G. Park, H. Shon, C. H. Ahn, and S. H. Kim, "Hybrid desalination processes for beneficial use of reverse osmosis brine: Current status and future prospects," *Desalination*, vol. 454, Elsevier B.V., pp. 104–111, Mar. 15, 2019, doi: 10.1016/j.desal.2018.02.002.
- [28] A. Almansoori and Y. Saif, "Structural optimization of osmosis processes for water and power production in desalination applications," *Desalination*, vol. 344, pp. 12–27, Jul. 2014, doi: 10.1016/J.DESAL.2014.03.002.
- [29] Minvivienda, "El plan nacional de desarrollo 2018-2022: 'Pacto por Colombia, pacto por la equidad,'" *Apuntes del Cenes*, 2019, doi: 10.19053/01203053.v38.n68.2019.9924.
- [30] H. Ritchie, "Global comparison: how much energy do people consume? - Our World in Data," 2021. Accessed: Jan. 31, 2022. [Online]. Available: <https://ourworldindata.org/per-capita-energy?country=>
- [31] IDEAM, *Evaluación Nacional del Agua 2018*. 2018.
- [32] O. Alvarez-Silva and A. F. Osorio, "Salinity gradient energy potential in Colombia considering site specific constraints," *Renew Energy*, vol. 74, pp. 737–748, Feb. 2015, doi: 10.1016/j.renene.2014.08.074.
- [33] R. Albrektiene, M. Rimeika, E. Zalieckiene, V. Šaulys, and A. Zagorskis, "Determination of Organic Matter by UV Absorption in the Ground Water," *Vilnius Gediminas Technical University*, vol. 20, no. 2, pp. 163–167, 2012, doi: 10.3846/16486897.2012.674039.
- [34] S. Loeb, "Production of energy from concentrated brines by pressure-retarded osmosis : I. Preliminary technical and economic correlations," *J Memb Sci*, vol. 1, no. C, pp. 49–63, Jan. 1976, doi: 10.1016/S0376-7388(00)82257-7.
- [35] N. Y. Yip and M. Elimelech, "Performance limiting effects in power generation from salinity gradients by pressure retarded osmosis," *Environ Sci Technol*, vol. 45, no. 23, pp. 10273–10282, Dec. 2011, doi: 10.1021/es203197e.
- [36] A. Achilli, T. Y. Cath, and A. E. Childress, "Power generation with pressure retarded osmosis: An experimental and theoretical investigation," *J Memb Sci*, vol. 343, no. 1–2, pp. 42–52, Nov. 2009, doi: 10.1016/J.MEMSCI.2009.07.006.
- [37] H. Sakai *et al.*, "Energy recovery by PRO in sea water desalination plant," *Desalination*, vol. 389, pp. 52–57, Jul. 2016, doi: 10.1016/J.DESAL.2016.01.025.

- [38] S. Xu, Y. Liu, Y. Wang, M. Zhang, Q. Xiao, and Y. Duan, "Influential analysis of concentration polarization on water flux and power density in PRO process: Modeling and experiments," *Desalination*, vol. 412, pp. 39–48, Jun. 2017, doi: 10.1016/J.DESAL.2017.02.020.